

# Phase covariant channel: Quantum speed limit of evolution

Riya Baruah,\* K.G. Paulson,† and Subhashish Banerjee‡

*Indian Institute of Technology, Jodhpur-342030, India*

(Dated: April 19, 2022)

The quantum speed of evolution for the phase covariant map is investigated. In this context, we consider various combinations of (non)-Markovian, CP-(in)divisible, quantum channels and analyze how they affect the quantum speed limit time. The role of coherence-mixedness balance on the speed limit time is checked in the presence of both vacuum and finite temperature effects. We also investigate how the combination of (non)-Markovian channels decides the rate at which Holevo's information changes under different purity conditions.

## I. INTRODUCTION

Nowadays, it's an established fact that one can manipulate the impact of quantum noise on quantum systems productively [1]. A good amount of work has been devoted to investigating the memory effects of noise on the dynamics of quantum systems [2–7]. In general, (non)-Markovianity discusses the nature of correlations that the system possesses with the environment. Quantum coherence and correlations are significant resources for quantum technology [8–12]. Non-Markovianity influences the quantum resources in both beneficial and unfavourable ways; consequently, the investigation of quantum correlation and coherence becomes highly significant [13–15]. Along with the memory effects on quantum resources, it is pertinent to discuss the evolution speed of quantum systems. It's been shown that energy-time uncertainty reveals the bound on the speed of the evolution of quantum states [16]. Initially, speed limit time was derived for the dynamics between the orthogonal states for isolated systems [17]. Later, quantum speed limit time for the time independent systems was extended to arbitrary mixed states [18]. Further, speed limit for the evolution between the states with arbitrary angle for a driven quantum system has been determined [19]. Recently, the speed of evolution between arbitrary states for open quantum systems [20–22] has become a lively research topic and is the central theme of the present work.

Not only from the dynamical perspective but also the system's characteristics revealed by the limit on the speed of evolution display its distinguishable role in quantum communication and technology. To list a few, the bound on speed limit time reveals how fast quantum information can be communicated, the maximum rate at which information can be processed, precision in quantum metrology [23–25], among others. Even though there exists no direct connection between non-Markovianity, a class of which is identified by information backflow and quantum speed

limit time ( $\tau_{QSL}$ ) [26], it's been shown that  $\tau_{QSL}$  could be realized as a witness of the decay-revival mechanism of quantum correlations [27] for a certain class of quantum noises. In [21, 28], it has been seen that quantum non-Markovianity speeds up the evolution of quantum states, which gives an operational definition to the CP-(in) divisible non-Markovian quantum channels. From the practical point of view,  $\tau_{QSL}$  finds a lot of applications in a wide range of fields [29].

In the present work, we estimate the  $\tau_{QSL}$  for single qubit states evolving under the phase covariant channel [30]. This channel can be thought of as an approximation of the general spin-Boson problem and involves both unital and non-unital components [31]. A work on similar lines was initiated recently in [32]. Here, in addition to the impact of various processes like heating, dissipation and dephasing on  $\tau_{QSL}$ , we also consider the role of coherence and mixing, as well as mixed initial states. Coherence is one of the central features of quantum physics [33]. Further, an open system evolution generally makes a system mixed. Hence, it is meaningful to ask how the balance between these two processes, *viz.* coherence and mixing, impacts the dynamics [15, 34]. We further consider different combinations of CP-(in)divisible (non)-Markovian quantum channels and a phenomenological model, and show how these combinations speed up quantum evolution for both pure and mixed initial states. The influence of thermal bath on  $\tau_{QSL}$ , along with the rate at which the upper bound for Holevo's information changes are also checked.

The present work is structured as follows. Section II discusses the prerequisites for the current work, which contains the details of the phase covariant channel, quantum speed limit, and the measure of non-Markovianity used here. In Sec. III, we investigate  $\tau_{QSL}$  and the impact of coherence-mixedness trade-off on  $\tau_{QSL}$  for different quantum phase covariant noises, for an initial pure state. Quantum speed limit time for an initially mixed state is discussed in Sec. IV, followed by concluding remarks in Sec. V.

\* baruah.1@iitj.ac.in

† paulsonkgeorg@gmail.com

‡ subhashish@iitj.ac.in

## II. PRELIMINARIES

Here we present the preliminary information required for this work. This begins with a brief overview of the phase covariant map, followed by a discussion of the quantum speed limit time using the geometric approach. Since, the interplay of coherence and mixing along with non-Markovian behaviour is central to the present work, these notions are then briefly introduced.

### A. The phase covariant map

The master equation for a single qubit phase covariant dynamics has the form [30]:

$$\begin{aligned} \frac{d\rho(t)}{dt} = & -i\frac{\omega(t)}{2}[\sigma_z, \rho(t)] + \frac{\gamma_1(t)}{2}\mathcal{L}_1(\rho(t)) + \frac{\gamma_2(t)}{2}\mathcal{L}_2(\rho(t)) \\ & + \frac{\gamma_3(t)}{2}\mathcal{L}_3(\rho(t)), \end{aligned} \quad (1)$$

where

$$\mathcal{L}_1(\rho(t)) = \sigma_+\rho(t)\sigma_- - \frac{1}{2}\{\sigma_-\sigma_+, \rho(t)\}, \quad (2)$$

$$\mathcal{L}_2(\rho(t)) = \sigma_-\rho(t)\sigma_+ - \frac{1}{2}\{\sigma_+\sigma_-, \rho(t)\}, \quad (3)$$

$$\mathcal{L}_3(\rho(t)) = \sigma_z\rho(t)\sigma_z - \rho(t), \quad (4)$$

and  $\sigma_{\pm} = (\sigma_x \pm i\sigma_y)/2$ . The action of the phase covariant map on an arbitrary single qubit density matrix  $\rho(0)$  is [35]:

$$\Phi_t(\rho(0)) = \rho(t) = \begin{pmatrix} 1 - p_1(t) & \alpha^*(t) \\ \alpha(t) & p_1(t) \end{pmatrix}, \quad (5)$$

where

$$p_1(t) = e^{-\Gamma(t)}[G(t) + p_1(0)], \quad (6)$$

$$\alpha(t) = \alpha(0)e^{i\Omega(t)-\Gamma(t)/2-\tilde{\Gamma}(t)}, \quad (7)$$

and

$$\Gamma(t) = \int_0^t \frac{\gamma_1(\tau) + \gamma_2(\tau)}{2} d\tau, \quad (8)$$

$$G(t) = \int_0^t e^{\Gamma(\tau)} \frac{\gamma_2(\tau)}{2} d\tau, \quad (9)$$

$$\Omega(t) = \int_0^t 2\omega(\tau) d\tau, \quad (10)$$

$$\tilde{\Gamma}(t) = \int_0^t \gamma_3(\tau) d\tau. \quad (11)$$

Here,  $\gamma_1(t)$ ,  $\gamma_2(t)$ ,  $\gamma_3(t)$  correspond to energy gain, energy loss and pure dephasing rates, respectively. Also  $\Omega(t)$  corresponds to rotations around the  $z$ -axis of the Bloch ball. Phase covariant dynamics for a single qubit satisfies the relation

$\exp(-i\sigma_z\phi)\Phi[\rho]\exp(i\sigma_z\phi) = \Phi[\exp(-i\sigma_z\phi)\rho\exp(i\sigma_z\phi)]$  for all real  $\phi$  [36]. It can be shown that phase covariant dynamics implies uniform deformation of the  $x$  and  $y$  Bloch vectors and permits a deformation as well as translation of the  $z$  Bloch vector.

### B. Quantum speed limit time

MT and ML-type bounds on speed limit time are estimated by using the geometric approach to quantify the closeness between the initial and final states. Here, Bures angle is used to measure the distance between two quantum states. In [21], for the initial pure state  $\rho_0 = |\psi_0\rangle\langle\psi_0|$ , a bound on the speed limit time based on Bures angle  $\mathcal{B}(\rho_0, \rho_t)$  is,

$$\tau_{QSL} = \max \left\{ \frac{1}{\Lambda_{\tau}^{\text{op}}}, \frac{1}{\Lambda_{\tau}^{\text{tr}}}, \frac{1}{\Lambda_{\tau}^{\text{hs}}} \right\} \sin^2[\mathcal{B}], \quad (12)$$

where  $\mathcal{B}(\rho_0, \rho_t) = \arccos(\sqrt{\langle\psi_0|\rho_t|\psi_0\rangle})$ , and  $\Lambda_{\tau}^{\text{op}}, \Lambda_{\tau}^{\text{tr}}$ , and  $\Lambda_{\tau}^{\text{hs}}$  are the operator, Hilbert-Schmidt and trace norms, respectively,

$$\Lambda_{\tau}^{\text{op,tr,hs}} = \frac{1}{\tau} \int_0^\tau dt \|\mathcal{L}(\rho_t)\|_{\text{op,tr,hs}}. \quad (13)$$

Operators satisfy the von Neumann trace inequality  $\|A\|_{\text{op}} \leq \|A\|_{\text{hs}} \leq \|A\|_{\text{tr}}$ , which gives,  $1/\Lambda_{\tau}^{\text{op}} \geq 1/\Lambda_{\tau}^{\text{hs}} \geq 1/\Lambda_{\tau}^{\text{tr}}$ . The tighter bound on the quantum speed limit time is achieved by using operator norm of the generator. An upper bound on fidelity for any density matrices  $\rho_1$  and  $\rho_2$  shows that [37]  $\mathcal{F}(\rho_1, \rho_2) \leq \text{tr}\rho_1\rho_2 + \sqrt{(1 - \text{tr}\rho_1^2)(1 - \text{tr}\rho_2^2)}$ . Making use of this super-fidelity, a bound on quantum speed limit time for both pure and mixed initial states can be written by multiplying the RHS in (Eq. 13) by a factor  $\left(1 + \sqrt{\frac{1 - \text{tr}\rho_0^2}{1 - \text{tr}\rho_t^2}}\right)$ .

### C. Coherence-mixing balance and the upper limit of the Holevo Bound

Mixedness of a quantum system imposes limits on the amount of quantum coherence it can possess [15, 38]. For a d-level system, this trade-off can be expressed as an inequality:

$$M_{cl} = \frac{C_{l_1}^2(\rho)}{(d-1)^2} + M_l(\rho) \leq 1. \quad (14)$$

For a two level system, using the density matrix equation Eq. (5), the trade-off equation can be shown to be in the following useful form

$$4p_1(t)(1 - p_1(t)) \leq 1, \quad (15)$$

see appendix for a detailed derivation. It was shown recently that the rate at which, accessible information,

quantified by the Holevo quantity  $\chi$  changes is upper bounded by the quantum speed limit time as [29], [39],

$$\dot{\chi} \leq \frac{\Delta\chi}{\tau_{QSL}}. \quad (16)$$

Here,  $\Delta\chi$  represents the change of  $\chi$ . This suggests that  $\tau_{QSL}$ , in particular,  $1/\tau_{QSL}$ , upper bounds the rate with which the accessible information changes.

#### D. Self similarity measure of non-Markovianity

Recently, a measure, which we call the SSS measure, was developed that approaches non-Markovian behaviour from the perspective of temporal self-similarity, the property of a system dynamics wherein the propagator between two intermediate states is independent of the initial time [40]. In particular, it quantifies non-Markovian behaviour in terms of deviation  $\zeta$  from temporal self-similarity

$$\zeta = \min_{\mathcal{L}^*} \frac{1}{T} \int_0^T \|\hat{\mathcal{L}}(t) - \hat{\mathcal{L}}^*\|_{\text{tr}} dt. \quad (17)$$

Here  $\|A\|_{\text{tr}} = \text{tr}\sqrt{A^\dagger A}$  is the trace norm of matrix  $A$ ,  $\hat{\mathcal{L}}(t)$  is the Lindbladian corresponding to the time-homogeneous master equation and  $\hat{\mathcal{L}}^*$  is a time-independent Lindblad generator.

### III. QUANTUM SPEED LIMIT TIME: ANALYSIS OF VARIOUS PHASE COVARIANT MAPS

Now, we study the phase covariant map using different rates, primarily in the non-Markovian region for single qubit pure states. We first characterise the non-Markovianity using the SSS measure, after which we calculate the  $\tau_{QSL}$  and study the trade-off between mixedness and coherence.

#### A. Non-Markovian amplitude damping and random telegraph noise

We consider here a combination of the non-unital non-Markovian amplitude damping (NMAD) and the unital random telegraph noise (RTN) dephasing channels [40]. Accordingly, we put  $\gamma_1(t) = 0$  in (1). For the NMAD channel,  $\gamma_2(t) = -\frac{4}{\Lambda(t)} \frac{d\Lambda(t)}{dt}$  where  $\Lambda(t) = e^{-lt/2}(\cosh(zt/2) + \frac{l}{z} \sinh(zt/2))$  [28] is the decoherence function. The decoherence rate then becomes

$$\gamma_2(t) = \frac{4\kappa l \sinh(zt/2)}{z \cosh(zt/2) + l \sinh(zt/2)}, \quad (18)$$

where  $z = \sqrt{l^2 - 2\kappa l}$ ,  $\kappa$  describes the qubit-environment coupling strength and  $l$  is the spectral width related to

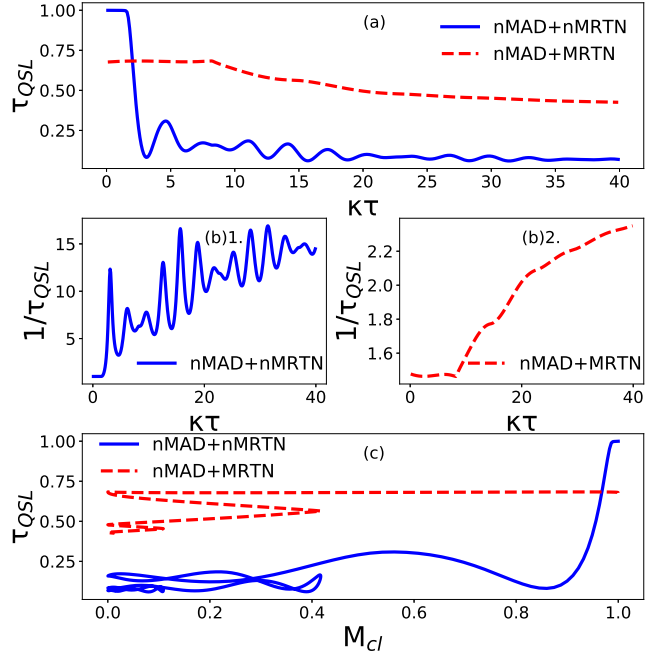


FIG. 1. (a) Quantum speed limit time  $\tau_{QSL}$  vs.  $\kappa\tau$  (b)  $\frac{1}{\tau_{QSL}}$  vs.  $\kappa\tau$  (c)  $\tau_{QSL}$  as a function of  $M_{cl}$  plotted for a combination of non-Markovian amplitude damping and RTN dephasing channels with  $\frac{1}{\sqrt{2}}(|0\rangle + |1\rangle)$  as the initial state.  $l = 0.1\kappa$ ,  $\alpha = \kappa$ .  $\eta = 0.1, 90$  for non-Markovian (nMRTN) and Markovian RTN (MRTN), respectively. Actual driving time  $\tau = 1$ .

the reservoir correlation time. The dynamics is Markovian in the region  $l > 2k$ , whereas it is non-Markovian in the region  $l < 2k$ . The dephasing rate for RTN is  $\gamma_3(t) = -\frac{1}{\Lambda(t)} \frac{d\Lambda(t)}{dt}$  where  $\Lambda(t) = e^{-\eta t}(\cos(\mu\eta t) + \frac{1}{\mu}\sin(\mu\eta t))$  and is

$$\gamma_3(t) = \frac{\eta(\mu^2 + 1) \sin(\mu\eta t)}{\mu \cos(\mu\eta t) + \sin(\mu\eta t)}, \quad (19)$$

where  $\mu = \sqrt{(\frac{2\alpha}{\eta})^2 - 1}$ . Here,  $\eta$  is the spectral band width and  $\alpha$  is the coupling strength between the qubit and the reservoir. Depending on whether  $(\frac{2\alpha}{\eta})^2 > 1$  or  $(\frac{2\alpha}{\eta})^2 < 1$ , the dynamics is non-Markovian or Markovian, respectively.

Using a similar combination of time independent amplitude damping and dephasing channels, an upper bound of the SSS measure can be calculated as,

$$\zeta = \int_0^T \|(2\gamma_2(t) - \kappa) \mathcal{L}_2 + 2\gamma_3(t) \mathcal{L}_3\|_{\text{tr}} dt. \quad (20)$$

Here the integration can be done numerically and  $\mathcal{L}_2$  and  $\mathcal{L}_3$  can be seen from Eqs. (2) and (3), respectively. Due to the time dependent nature of the rates,  $\zeta > 0$  indicating the presence of memory. Fig. 1(a) depicts the behaviour of  $\tau_{QSL}$  with respect to the dimensionless time ( $\kappa\tau$ ) involving the coupling strength ( $\kappa$ ) for the maximally coherent initial state  $\frac{1}{\sqrt{2}}(|0\rangle + |1\rangle)$ . We find that a more

non-Markovian combination of channels generally leads to a lower  $\tau_{QSL}$  as we increase the coupling strength. This suggests that the non-markovianity of the evolution aids in the speeding up of the dynamics as well as in increasing the accessible information. The  $\tau_{QSL}$  vs. the  $M_{cl}$  plot brings out the influence of coherence and mixing on the quantum speed. The nature of the curve reflects the range of coupling strength taken in the figures. The oscillatory nature of the curves could be attributed to the RTN noise in the non-Markovian regime.

### B. Non-Markovian amplitude damping and modified Ornstein–Uhlenbeck noise

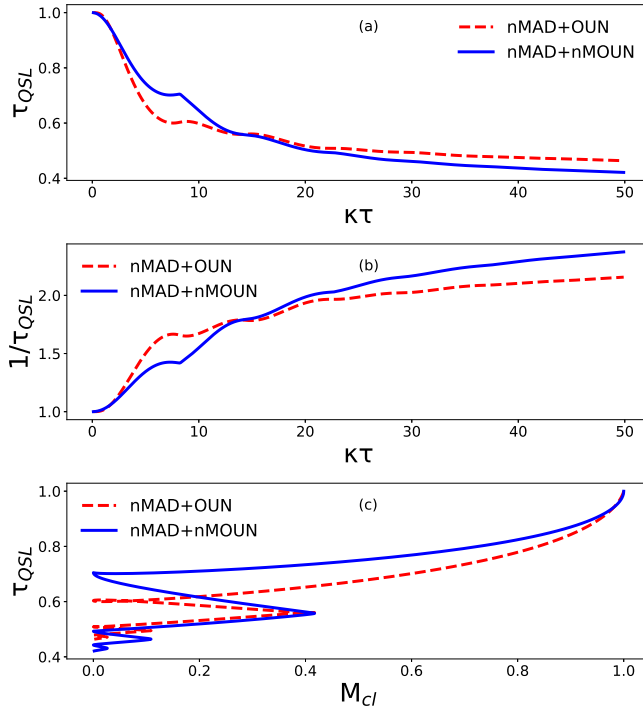


FIG. 2. (a) Quantum speed limit time  $\tau_{QSL}$  vs.  $\kappa\tau$  (b)  $\frac{1}{\tau_{QSL}}$  vs.  $\kappa\tau$  (c)  $\tau_{QSL}$  as a function of  $M_{cl}$  plotted for a combination of non-Markovian amplitude damping and OUN dephasing channels with  $\frac{1}{\sqrt{2}}(|0\rangle + |1\rangle)$  as the initial state.  $m = l = 0.1\kappa$ .  $p = 10$  for both OUN (Markovian) and nMOUN (non-Markovian).

Modified Ornstein-Uhlenbeck noise OUN is CP divisible but it is still non-Markovian as it exhibits memory effects as captured by the SSS measure [40]. The OUN dephasing rate is  $\gamma_3(t) = -\frac{1}{\Lambda(t)} \frac{d\Lambda(t)}{dt}$  where  $\Lambda(t) = \exp(-\frac{p}{2}(t + \frac{1}{m}(e^{-mt} - 1)))$  which is calculated as

$$\gamma_3(t) = \frac{p}{2}(1 - e^{-mt}). \quad (21)$$

Here,  $p$  is the inverse of the effective relaxation time and  $m$  is related to the noise band width. This channel is Markovian in the limit  $\frac{1}{m} \rightarrow \infty$  for which case

$\Lambda(t) = e^{-pt/2}$  and  $\gamma_3(t) = p/2$ . We use Eq. (18) for  $\gamma_2(t)$  and  $\gamma_1(t) = 0$ .

The upper bound of the SSS measure for a combination of NMAD and OUN is estimated to be

$$\zeta = \int_0^T \left\| (2\gamma_3(t) - \kappa) \mathcal{L}_2 - \frac{pe^{-mt}}{2} \mathcal{L}_3 \right\|_{\text{tr}} dt. \quad (22)$$

Similar to the previous case,  $\zeta > 0$ . These channels exhibit memory effects. The variation of  $\tau_{QSL}$  for OUN in combination with NMAD with respect to coupling strength is depicted in Fig. 2(a) for the initial maximally coherent state. The behaviour of  $\tau_{QSL}$  changes depending on the OUN parameters chosen, with the more non-Markovian combination having a lower  $\tau_{QSL}$  in certain conditions, as depicted in Fig. 2(a). This feature could be attributed to the CP divisible nature of the modified OUN noise considered here. It also brings out that, in general, with the increase in memory, the evolution speeds up. This translates into the upper bound of the Holevo rate, as illustrated in Fig. 2(b). Corresponding to the same initial state, we see the different trajectories taken by the tradeoff between mixedness and coherence in Fig. 2(c). The multiple values of  $\tau_{QSL}$  for the same  $M_{cl}$  is suggestive of the information backflow inherent in the dynamics.

### C. A phenomenological model

Here, we consider a model which is CP, uses all the rates  $\gamma_1(t)$ ,  $\gamma_2(t)$  and  $\gamma_3(t)$  and reproduces the Markovian master equation in the appropriate limit [41]. The decay rates are given as

$$\gamma_1(t) = 2\mathcal{N}f(t), \quad (23)$$

$$\gamma_2(t) = 2(\mathcal{N} + 1)f(t), \quad (24)$$

where

$$f(t) = -2\text{Re} \left\{ \frac{1}{c(t)} \frac{dc(t)}{dt} \right\}, \quad (25)$$

$$c(t) = c(0)e^{-t/2} \left[ \cosh(\sqrt{1-2R}t/2) + \frac{\sinh(\sqrt{1-2R}t/2)}{\sqrt{1-2R}} \right]. \quad (26)$$

$R$  is a dimensionless constant greater than zero and depicts the coupling between the system and the environment as well as the environmental spectral properties.  $\mathcal{N}(T) = [\exp(\hbar\nu_0/k_B T) - 1]^{-1}$  is the mean number of excitations in the modes of the thermal environment, where  $T$  is the temperature and  $\nu_0$  is the Bohr frequency. When  $R < 1/2$ ,  $\gamma_1(t)$  and  $\gamma_2(t)$  are always positive. They become negative for certain time intervals when  $R > 1/2$  and the dynamics becomes non-Markovian. At temperature  $T = 0$ ,  $\mathcal{N}(T) = 0$  and it reduces to non-Markovian amplitude damping. This matches with  $\gamma_2(t)$  in Eq. (18) with  $l$  equal to one. The pure dephasing rate is given by

$$\gamma_3(t) = 2 \int d\omega J(\omega) \coth(\omega/k_B T) \sin(\omega t), \quad (27)$$

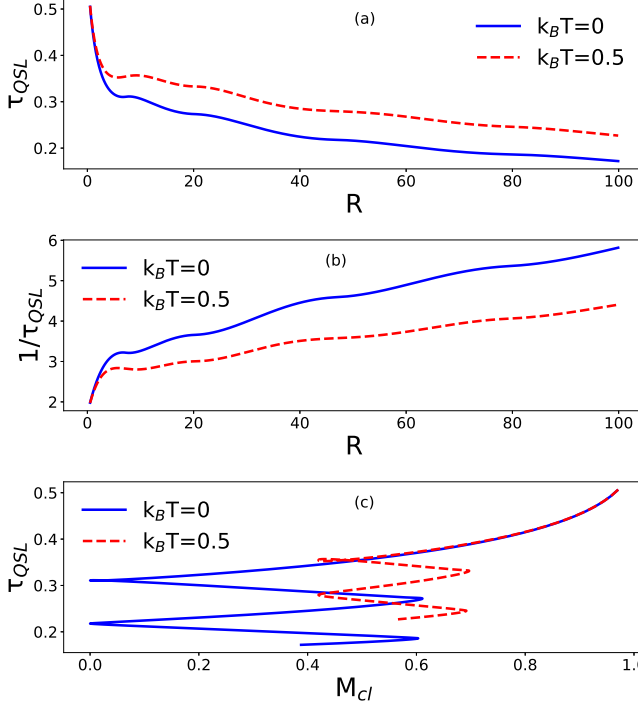


FIG. 3. (a) Quantum speed limit time  $\tau_{QSL}$  vs.  $R$  (b)  $\frac{1}{\tau_{QSL}}$  vs.  $R$  where  $R>0.5$  (c)  $\tau_{QSL}$  as a function of  $M_{cl}$  plotted for the temperature dependent decay and dephasing processes at temperatures  $k_B T = 0, 0.5$  for super ohmic spectral density  $s=4$ .  $\frac{1}{\sqrt{2}}(|0\rangle + |1\rangle)$  is the initial state taken.  $c(0)=1$ ,  $\omega_c = 1$ ,  $v = 1$ . Actual driving time  $\tau = 1$

where the spectral density  $J(\omega)$  is

$$J(\omega) = \frac{v\omega^s}{\omega_c^s} e^{-\omega/\omega_c}, \quad (28)$$

with  $\omega_c$  being the cut off frequency and  $v$  is a dimensionless constant. In the pure dephasing case, i.e., when  $\gamma_1(t) = \gamma_2(t) = 0$ , the Ohmic parameter  $s$  as a function of temperature determines the Markovianity of the model. The system is non-Markovian when  $s > s_{crit}(T)$ . The critical value of  $s$  has a minimum of  $s_{crit}(0) = 2$  at  $T = 0$  and a maximum of  $s_{crit}(T \rightarrow \infty) = 3$  in the high temperature limit.

The upper bound of the SSS measure for this model is as

$$\zeta = \int_0^T \|2\gamma_1(t)\mathcal{L}_1 + 2\gamma_2(t)\mathcal{L}_2 + 2\gamma_3(t)\mathcal{L}_3\|_{tr} dt. \quad (29)$$

This turns out to be a positive quantity for  $T>0$ , indicating the presence of memory.

With the maximally coherent state taken as the initial state, Fig. 3(a) shows the behaviour of  $\tau_{QSL}$  with respect to  $R$ . We find that that  $\tau_{QSL}$  is higher at finite temperatures and continues to increase with the increase in temperature. The increase in temperature has a tendency of slowing down the process. Correspondingly, upper bound of the Holevo information is larger for lower

temperatures, as depicted in Fig. 3(b). Figure 3(c) shows the trajectories taken by the  $\tau_{QSL}$  with respect to  $M_{cl}$  at different temperatures. At finite temperatures, the system never reaches a pure state corresponding to  $M_{cl} = 0$ .

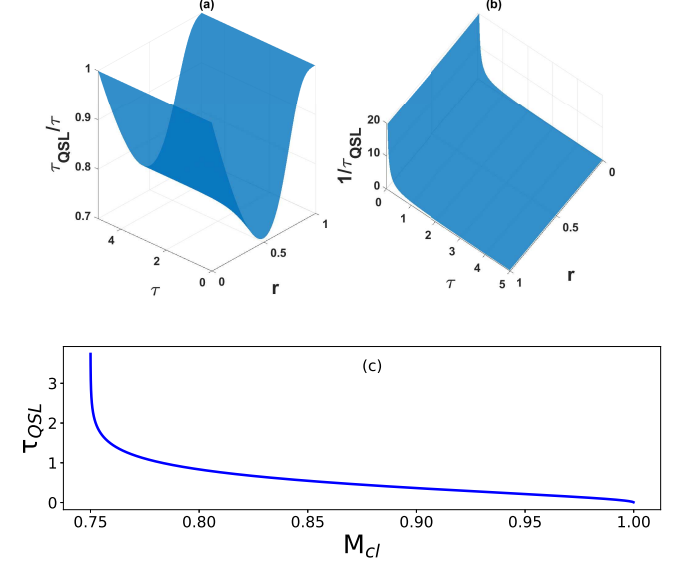


FIG. 4. (a)  $\tau_{QSL}/\tau$  and (b)  $1/\tau_{QSL}$  with respect to  $\tau$  and  $r$ , (c)  $\tau_{QSL}$  plotted as a function of  $M_{cl}$  with the maximally coherent state taken as the initial state for eternal CP-indivisible dynamics. Here  $b = 0.5$ ,  $\nu = 1$ .

#### D. Eternally CP-indivisible dynamics

A family of non-unital eternal CP-indivisible dynamical maps with the decay rates

$$\gamma_1(t) = 2\nu(1+b), \quad (30)$$

$$\gamma_2(t) = 2\nu(1-b), \quad (31)$$

$$\gamma_3(t) = -\frac{\nu(1-b^2)\sinh(2\nu t)}{[1+b^2+(1-b^2)\cosh(2\nu t)]}, \quad (32)$$

was introduced in [36]. Here,  $\nu > 0$ . When  $|b| < 1$ ,  $\gamma_3(t) < 0$  for all  $t>0$ .

The upper bound of the SSS measure for this channel is

$$\zeta = \frac{1}{T} \ln \left( \frac{1+b^2+(1-b^2)\cosh(2\nu T)}{2} \right). \quad (33)$$

As  $\zeta > 0$  for  $T > 0$ , we see that this channel possesses memory. In Fig. 4(a), we plot  $\tau_{QSL}$  as a function of  $\tau$ , the driving time and  $r$ , where  $r$  is used to parameterize the single qubit wavefunction,  $|\psi\rangle = \sqrt{r}|0\rangle + \sqrt{1-r}|1\rangle$ . Depending on the initial state chosen, behaviour of  $\tau_{QSL}$  varies. We find  $\tau_{QSL}/\tau = 1$  for two different states, when  $r = 0$  and when  $r = 1$ , while for all other states, it remains below 1. The upper bound to the Holevo rate decreases rapidly with the increase in driving time for all

states, as can be seen in Fig. 4(b). The  $\tau_{QSL}$  is plotted as a function of  $M_{cl}$  in Fig. 4(c). With the maximally coherent state taken as the initial state,  $M_{cl}$  first decreases from 1 as  $\tau_{QSL}$  increases and then remains steady at 0.75 in Fig. 4(c). This can be explained using Eq. (15). In the limit  $\tau \rightarrow \infty$ , we find  $M_{cl} = (1 - b^2)$  which is equal to 0.75 for our chosen  $b = 0.5$ .

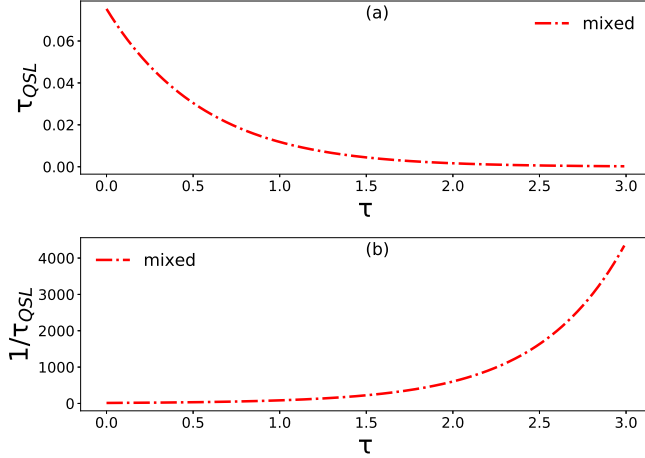


FIG. 5. (a)  $\tau_{QSL}$  and (b)  $1/\tau_{QSL}$  plotted with respect to  $\tau$  for the eternally CP-indivisible channel. The initial mixed state has purity  $(\text{tr}(\rho^2))$  of 0.56 with  $r_x = r_y = r_z = 0.2$ . Here  $\tau_d = 1$ ,  $b = 0.5$  and  $\nu = 1$ .

#### IV. INITIAL MIXED STATES

So far, we have considered only initial pure states. In this section, we calculate the quantum speed limit time using initial mixed states for the eternal CP-indivisible dynamics. The single qubit density matrix is

$$\rho = \frac{1}{2} \begin{pmatrix} 1 + r_z & r_x - ir_y \\ r_x + ir_y & 1 - r_z \end{pmatrix}, \quad (34)$$

where  $|r| \leq 1$  with the inequality for mixed states. The time evolved density matrix for the eternally CP-indivisible channel then becomes,

$$\rho(t) = \frac{1}{2} \begin{bmatrix} 1 + e^{-2\nu t} (r_z + b(e^{2\nu t} - 1)) & (r_x - ir_y) e^{-2vt} \sqrt{\frac{1+b^2+(1-b^2\cosh(2\nu t))}{2}} \\ (r_x + ir_y) e^{-2vt} \sqrt{\frac{1+b^2+(1-b^2\cosh(2\nu t))}{2}} & 1 - e^{-2\nu t} (r_z + b(e^{2\nu t} - 1)) \end{bmatrix}. \quad (35)$$

We use the modified  $\tau_{QSL}$  with the factor  $\left(1 + \sqrt{\frac{1-\text{tr}\rho_\tau^2}{1-\text{tr}\rho_t^2}}\right)$  multiplied to Eq. (13). We look for the minimal time required for the system to evolve from a mixed initial state  $\rho_\tau$  to the final state  $\rho_{\tau+\tau_d}$ . As the open system quantum evolution is non-unitary,  $\rho_{\tau+\tau_d}$  is also a mixed state. The modified  $\tau_{QSL}$  is

$$\tau_{QSL} = \frac{\sin^2[\mathcal{B}_{\tau,\tau+\tau_d}]}{\frac{1}{\tau_d} \int_\tau^{\tau+\tau_d} dt \|\mathcal{L}(\rho_t)\|_{\text{op}} \left(1 + \sqrt{\frac{1-\text{tr}\rho_\tau^2}{1-\text{tr}\rho_t^2}}\right)}, \quad (36)$$

where  $\mathcal{B}_{\tau,\tau+\tau_d} = \arccos(\mathcal{F}(\rho_\tau, \rho_{\tau+\tau_d}))$  and  $\mathcal{F}$  is the super fidelity. Using this definition,  $\tau_{QSL}$  is plotted in Fig. 5(a) as a function of the driving time  $\tau$  with  $\tau_d = 1$ .  $\tau_{QSL}$  and  $1/\tau_{QSL}$  are plotted in Figs. 5(a) and (b), respectively. They indicate that with evolution, the minimum time required to achieve a particular overlap between two mixed states decreases.

#### V. CONCLUSION

An exhaustive study of  $\tau_{QSL}$  for the phase covariant channel was made. In this context, various combinations of non-Markovian channels were used, ranging from the CP-divisible to CP-indivisible and P-indivisible. Both, initially pure as well as mixed states were studied. Analysis of the quantum speed limit time for combinations of Markovian and non-Markovian channels reveals how fast or slow the underlying dynamics is. For the initial maximally coherent state, it was found that a combination of CP-indivisible channels generally results in lower  $\tau_{QSL}$ . This suggests that the non-Markovianity of the evolution aids in the speeding up of the dynamics as well as in increasing the accessible information. In the phenomenological model, temperature was found to affect  $\tau_{QSL}$  significantly, with  $\tau_{QSL}$  increasing with the increase in temperature for the chosen initial state. Another feature of this study is the impact of the coherence-mixedness trade-off on  $\tau_{QSL}$ , for evolutions generated by the phase-covariant map in general. Various features of

the dynamics such as information backflow, temperature effects could be ascertained from this. The generality of the present study implies that special cases of the phase-covariant map, such as the amplitude damping and the pure dephasing channels, can be easily obtained as simplifications of the models studied.

## ACKNOWLEDGEMENT

SB acknowledges support from the Interdisciplinary Cyber-Physical Systems (ICPS) programme of the Department of Science and Technology (DST), India, Grant No.: DST/ICPS/QuST/Theme-1/2019/6. SB also acknowledges support from the Interdisciplinary Program (IDRP) on Quantum Information and Computation (QIC) at IIT Jodhpur.

---

[1] S. Banerjee, *Open Quantum Systems: Dynamics of Non-classical Evolution*, Vol. 20 (Springer, 2018).

[2] Á. Rivas, S. F. Huelga, and M. B. Plenio, *Reports on Progress in Physics* **77**, 094001 (2014).

[3] L. Li, M. J. Hall, and H. M. Wiseman, *Physics Reports* **759**, 1 (2018).

[4] H.-P. Breuer, E.-M. Laine, J. Piilo, and B. Vacchini, *Rev. Mod. Phys.* **88**, 021002 (2016).

[5] N. P. Kumar, S. Banerjee, R. Srikanth, V. Jagadish, and F. Petruccione, *Open Systems & Information Dynamics* **25**, 1850014 (2018).

[6] U. Shrikant, R. Srikanth, and S. Banerjee, *Phys. Rev. A* **98**, 032328 (2018).

[7] A. Ghosal, D. Das, and S. Banerjee, *Phys. Rev. A* **103**, 052422 (2021).

[8] K. G. Paulson and S. V. M. Satyanarayana, *Quant. Inf. Compt.*, **14**, 1227 (2014).

[9] G. Adesso, T. R. Bromley, and M. Cianciaruso, *Journal of Physics A: Mathematical and Theoretical* **49**, 473001 (2016).

[10] A. Streltsov, G. Adesso, and M. B. Plenio, *Reviews of Modern Physics* **89**, 041003 (2017).

[11] K. Paulson and P. K. Panigrahi, *Physical Review A* **100**, 052325 (2019).

[12] F. Sapienza, F. Cerisola, and A. J. Roncaglia, *Nature communications* **10**, 1 (2019).

[13] K. Thapliyal, A. Pathak, and S. Banerjee, *Quantum Information Processing* **16**, 1 (2017).

[14] S. Utagi, R. Srikanth, and S. Banerjee, *Quantum Inf. Process.* **19**, 366 (2020).

[15] S. Bhattacharya, S. Banerjee, and A. K. Pati, *Quantum Information Processing* **17**, 1 (2018).

[16] L. Mandelstam and I. Tamm, *J.Phys* **9**, 249 (1945).

[17] N. Margolus and L. B. Levitin, *Physica D: Nonlinear Phenomena* **120**, 188 (1998).

[18] V. Giovannetti, S. Lloyd, and L. Maccone, *Physical Review A* **67**, 052109 (2003).

[19] S. Deffner and E. Lutz, *Journal of Physics A: Mathematical and Theoretical* **46**, 335302 (2013).

[20] A. del Campo, I. L. Egusquiza, M. B. Plenio, and S. F. Huelga, *Physical review letters* **110**, 050403 (2013).

[21] S. Deffner and E. Lutz, *Phys. Rev. Lett.* **111**, 010402 (2013).

[22] M. M. Taddei, B. M. Escher, L. Davidovich, and R. L. de Matos Filho, *Phys. Rev. Lett.* **110**, 050402 (2013).

[23] J. D. Bekenstein, *Physical Review Letters* **46**, 623 (1981).

[24] S. Lloyd, *Nature* **406**, 1047 (2000).

[25] V. Giovannetti, S. Lloyd, and L. Maccone, *Nature photonics* **5**, 222 (2011).

[26] J. Teittinen, H. Lyyra, and S. Maniscalco, *New Journal of Physics* **21**, 123041 (2019).

[27] K. Paulson, E. Panwar, S. Banerjee, and R. Srikanth, *Quantum Information Processing* **20**, 1 (2021).

[28] K. Paulson, S. Banerjee, and R. Srikanth, arXiv preprint arXiv:2107.03306 (2021).

[29] S. Deffner and S. Campbell, *Journal of Physics A: Mathematical and Theoretical* **50**, 453001 (2017).

[30] A. Smirne, J. Kołodyński, S. F. Huelga, and R. Demkowicz-Dobrzański, *Physical review letters* **116**, 120801 (2016).

[31] J. F. Haase, A. Smirne, J. Kołodyński, R. Demkowicz-Dobrzański, and S. F. Huelga, *New Journal of Physics* **20**, 053009 (2018).

[32] J. Teittinen and S. Maniscalco, *Entropy* **23**, 331 (2021).

[33] T. Baumgratz, M. Cramer, and M. B. Plenio, *Phys. Rev. Lett.* **113**, 140401 (2014).

[34] K. Dixit, J. Naikoo, S. Banerjee, and A. K. Alok, *The European Physical Journal C* **79**, 1 (2019).

[35] J. Teittinen, H. Lyyra, B. Sokolov, and S. Maniscalco, *New Journal of Physics* **20**, 073012 (2018).

[36] S. N. Filippov, A. N. Glinov, and L. Leppäjärvi, *Lobachevskii Journal of Mathematics* **41**, 617–630 (2020).

[37] J. A. Miszczak, Z. Puchała, P. Horodecki, A. Uhlmann, and K. Życzkowski, *Quantum Inf. Comput.* **9**, 103 (2009).

[38] U. Singh, M. N. Bera, H. S. Dhar, and A. K. Pati, *Phys. Rev. A* **91**, 052115 (2015).

[39] T. V. Accocia and S. Deffner, arXiv preprint arXiv:1706.03826 (2017).

[40] S. Utagi, R. Srikanth, and S. Banerjee, *Scientific Reports* **10**, 1 (2020).

[41] J. Lankinen, H. Lyyra, B. Sokolov, J. Teittinen, B. Ziae, and S. Maniscalco, *Phys. Rev. A* **93**, 052103 (2016).

## Appendix A:

The  $l_1$  norm of coherence is given by:

$$C_{l_1} = \sum_{i \neq j} |\rho_{ij}|. \quad (\text{A1})$$

For a qubit, this is the sum of the absolute value of the off-diagonal elements. The mixedness, based on normalized linear entropy for a single qubit is:

$$M_l(\rho) = 2(1 - \text{Tr}(\rho^2)). \quad (\text{A2})$$

Using (5), (A1) and (A2), we find for the phase covariant noise:

$$C_{l_1} = 2|\alpha(t)|, \quad (\text{A3})$$

$$M_l(\rho) = 4(p_1(t) - p_1(t)^2 - |\alpha(t)|^2). \quad (\text{A4})$$

The trade-off between mixedness and coherence ( $C_{l_1}^2 + M_l(\rho) := M_{cl}$ ) is then calculated as:

$$M_{cl} = 4p_1(t)(1 - p_1(t)) \leq 1. \quad (\text{A5})$$